[CANCER RESEARCH 64, 440–445, January 15, 2004]

Advances in Brief

Slippage of Mitotic Arrest and Enhanced Tumor Development in Mice with *BubR1* Haploinsufficiency

Wei Dai,[1] Qi Wang,[1] Tongyi Liu,[1] Malisetty Swamy,[4] Yuqiang Fang,[1] Suqing Xie,[1] Radma Mahmood,[2] Yang-Ming Yang,[1] Ming Xu,[3] and Chinthalapally V. Rao[4]

[1]Division of Molecular Carcinogenesis, Department of Medicine, New York Medical College, Valhalla, New York; [2]Core Facility for Histopathology, Albert Einstein College of Medicine, Bronx, New York; [3]Department of Cell Biology, University of Cincinnati College of Medicine, Cincinnati, Ohio; and [4]Institute for Cancer Prevention, Valhalla, New York

Abstract

A compromised spindle checkpoint is thought to play a key role in genetic instability that predisposes cells to malignant transformation. Loss of function mutations of BubR1, an important component of the spindle checkpoint, have been detected in human cancers. Here we show that *BubR1*$^{+/-}$ mouse embryonic fibroblasts are defective in spindle checkpoint activation, contain a significantly reduced amount of securin and Cdc20, and exhibit a greater level of micronuclei than do wild-type cells. RNA interference-mediated down-regulation of BubR1 also greatly reduced securin level. Moreover, compared with wild-type littermates, *BubR1*$^{+/-}$ mice rapidly develop lung as well as intestinal adenocarcinomas in response to challenge with carcinogen. BubR1 is thus essential for spindle checkpoint activation and tumor suppression.

Introduction

The spindle checkpoint functions to block the anaphase entry until each of every condensed chromosome has successfully attached to the spindle microtubules. Vertebrate BubR1 plays a key role in spindle checkpoint activation, during which it is extensively phosphorylated (1). Hyperphosphorylated BubR1 and other components of the checkpoint machinery, including Bub1, Bub3, Mad1, Mad2, and CENP-E, are associated with unattached kinetochores (2, 3). Although it appears that BubR1 and Mad2 may function in a single pathway after spindle checkpoint activation (4), BubR1 is a much more potent inhibitor of the anaphase-promoting complex (APC) than is Mad2 (5). A recent study shows that spindle checkpoint activation or silencing is mediated through CENP-E-dependent activation or inactivation of BubR1 kinase (6). A loss of spindle checkpoint function is thought to contribute to the development of cancer because of its role in maintaining genomic stability (7). Indeed, aneuploidy is prevalent in many types of cancer. Although the physiological and molecular basis of this abnormality remains unclear, recent studies indicate that chromosomal instability is closely associated with the loss of a functional spindle checkpoint (7). Mutations in *BubR1* have been detected in colonic cancers (8). In addition, a recent study has shown that *BubR1* is epigenetically down-regulated in a substantial fraction of human cancers (9). To determine the physiological function of BubR1, we have generated *BubR1* mutant mice. Mouse embryonic fibroblasts (MEFs) from *BubR1*$^{+/-}$ animals were found to contain lower levels of securin and Cdc20 as well as BubR1 than MEFs from wild-type embryos. *BubR1* deficiency resulted in mitotic slippage and formation of micronuclei at an enhanced rate. Moreover, *BubR1*$^{+/-}$ animals were prone to rapid development of tumors in multiple organs after exposure to a carcinogen.

Materials and Methods

Immunoblot Analysis. MEFs or HeLa cells were suspended in a lysis buffer (1), and the cell lysates were centrifuged at 12,000 × *g* for 10 min at 4°C. Equal amounts of proteins were then subjected to SDS-PAGE and immunoblot analysis with antibodies to BubR1, securin (Novocastra), Mad2, Cdc20, Plk3, or α-tubulin (Sigma). Immune complexes were detected with an appropriate second antibody conjugated with horseradish peroxidase (Sigma) and enhanced chemiluminescence reagents (Amersham Pharmacia Biotech).

Fluorescence Microscopy and Immunohistochemistry. Cells fixed in methanol were treated with 0.1% Triton X-100 on ice and then washed three times with ice-cold PBS. After blocking with 2.0% BSA in PBS for 15 min on ice, cells were incubated for 1 h with antibodies to BubR1, α-tubulin, or CREST; washed with PBS; and then incubated with appropriate second antibodies conjugated with Rodamine-Red-X or FITC (Jackson ImmunoResearch). Cells were finally stained with 4′,6-diamidino-2-phenylindole (1 μg/ml; Fluka). Fluorescence microscopy was performed on a Nikon microscope, and images were captured using a digital camera (Optronics). Immunohistochemistry was performed using a kit purchased from Vector Laboratory according to the instructions provided by the supplier.

RNA Interference. Double-stranded RNAs of 21 nucleotides in length were synthesized by Dharmacon Research. The targeting sequence was 5′-AAGGGAAGCCGAGCUGUUGAC-3′, corresponding to the coding region of 1281–1301 in human *BubR1* (accession number AF068760 GenBank) and 1259–1279 in mouse *BubR1* (accession number NM009773 GenBank) relative to the first nucleotide of ATG start codon. The control small interfering RNA (siRNA) targets luciferase mRNA (accession number X65324) of the firefly (*Photinus pyralis*), and the targeting sequence was 5′-UUCCTACGCTGAGTACTTCGA-3′ (GL-3; Dharmacon Research). Double nucleotides (dTdT) were added at the 3′ end of each strand. RNA duplexes were transfected into HeLa cells via the Oligofectamine approach (Invitrogen).

Mouse Carcinogenesis Assay. At 6 weeks of age, female mice (10 wild-type and 10 *BubR1*$^{+/-}$) were fed semipurified AIN-76A diets. One week after initiation of diets, both groups of mice were given s.c. azoxymethane (AOM; 4 mg/kg body weight) two times weekly for 4 weeks. All animals were weighed once every 2 weeks until termination of the study. Eight or 12 weeks after carcinogen treatment, mice were sacrificed by CO_2 euthanasia, and their colons were removed and flushed with Krebs Ringer solution. The dissected colons were opened and fixed flat between two pieces of filter paper in 10% buffered formalin for microadenoma analysis. After a minimum of 24 h in buffered formalin, the colons were cut into segments and placed in a Petri dish containing 0.2% methylene blue in Krebs Ringer solution. They were then placed mucosal side up on a microscope slide and observed through a light microscope. The colon microadenomas present were scored according to standard procedures that are being used routinely in our laboratory (10). Colons showing adenoma-like masses were fixed and subjected to histological analysis after H&E staining.

Results

To study the consequence of loss of *BubR1* function on genetic instability and tumor formation, we have generated *BubR1* mutant

Received 10/03/03; revised 11/15/03; accepted 11/26/03.

Grant support: NIH Grants RO1-CA90658 (to W. D.) and RO1-CA80003 (to C. V. R.).

The costs of publication of this article were defrayed in part by the payment of page charges. This article must therefore be hereby marked *advertisement* in accordance with 18 U.S.C. Section 1734 solely to indicate this fact.

Requests for reprints: Wei Dai, Division of Molecular Carcinogenesis, Department of Medicine, New York Medical College, Valhalla, New York 10595.

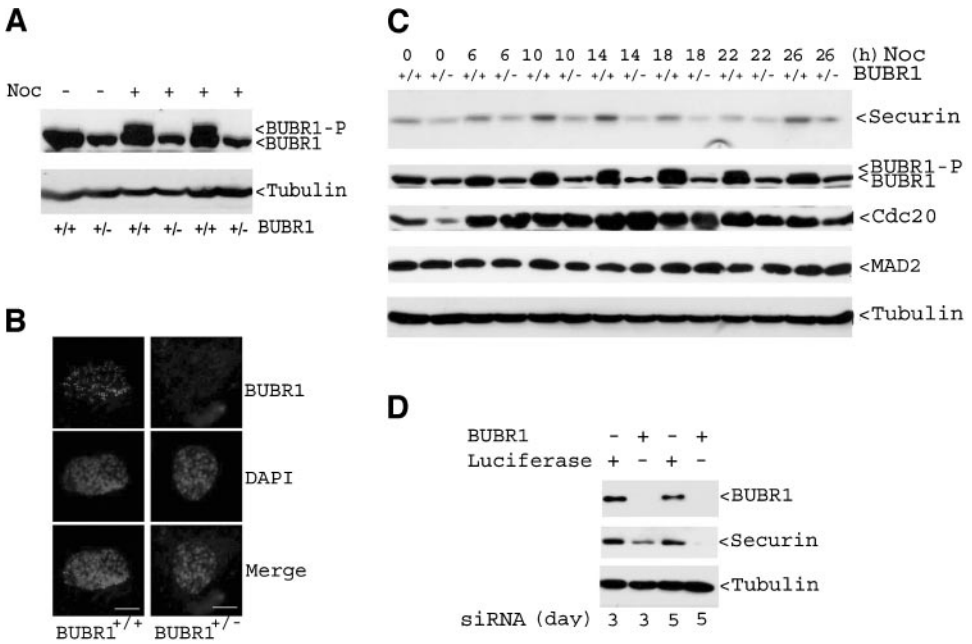

Fig. 1. Compromised spindle checkpoint function in *BubR1*$^{+/-}$ mouse embryonic fibroblasts (MEFs). *A*, wild-type and *BubR1*$^{+/-}$ MEF cells were incubated in the absence or presence (with a duplicate) of nocodazole (*Noc*; 0.5 μg/ml) for 16 h, after which cell lysates were prepared and subjected to immunoblot analysis with antibodies to BubR1 or to α-tubulin. BubR1-P denotes phosphorylated BubR1. *B*, wild-type and *BubR1*$^{+/-}$ MEF cells were fixed and stained with the antibody to BubR1 (*green*), and DNA was stained with 4′,6-diamidino-2-phenylindole (*blue*). A representative prophase cell from either cell type is shown. *Bar*, 2 μm. *C*, *BubR1*$^{+/-}$ and wild-type MEFs were incubated with nocodazole (0.5 μg/ml) for the indicated times, after which equal amounts of cell lysates were subjected to immunoblot analysis with antibodies to securin, BubR1, Mad2, Cdc20, or α-tubulin. Data in all panels are representative of at least three independent experiments. *D*, HeLa cells transfected with small interfering RNA (siRNA) for 3 or 5 days were assayed for BubR1, securin, or α-tubulin expression via immunoblotting.

mice (11). *BubR1* deficiency results in early embryonic death (11). To confirm that *BubR1*$^{+/-}$ cells actually contained a reduced level of BubR1, we examined the abundance of BubR1 in MEFs derived from embryonic day 14.5 embryos produced from intercrosses of *BubR1*$^{+/-}$ mice. The genotype of each MEF line was determined by nested PCR (11). Immunoblot analysis revealed that the amount of BubR1 in *BubR1*$^{+/-}$ MEFs was less than that in wild-type MEFs (Fig. 1*A*). Interestingly, the average level of BubR1 in *BubR1*$^{+/-}$ MEFs was about 25% (rather than the expected 50%) of that in wild-type MEFs (data not shown). This greatly reduced level of BubR1 apparently failed to accumulate at kinetochores during early mitosis (Fig. 1*B*), suggesting that BubR1 in *BubR1*$^{+/-}$ MEFs may not be efficiently activated. Indeed, exposure to the spindle checkpoint activator nocodazole for 16 h resulted in an apparent upshift of BubR1 due to phosphorylation[1] in wild-type MEFs but not in *BubR1*$^{+/-}$ MEFs (Fig. 1*A*). Thus, ablation of one *BubR1* allele apparently reduced the expression of the other allele, and the reduced level of BubR1 also compromised its activation after microtubule disruption.

BubR1 functions as a potent inhibitor of APC during activation of the spindle checkpoint (5). Metaphase and anaphase transition requires the destruction of securin in an APC-dependent manner. Cells with a compromised spindle checkpoint would be expected to exhibit increased APC activity and a consequent reduced abundance of securin. Indeed, immunoblot analysis revealed that the amount of securin in cycling *BubR1*$^{+/-}$ MEFs was reduced compared with that in wild-type cells. Although nocodazole induced a slight accumulation of securin in *BubR1*$^{+/-}$ MEFs, the steady-state level of this protein was much lower in these cells than in wild-type MEFs treated with nocodazole for the same time (Fig. 1*C*), consistent with the notion that *BubR1*$^{+/-}$ cells are defective in spindle checkpoint control. In addition, the abundance of Cdc20 was low in cycling *BubR1*$^{+/-}$ MEFs. On nocodazole treatment, Cdc20 was greatly increased in these cells. The kinetics of Cdc20 increase in *BubR1*$^{+/-}$ MEFs was similar to that observed in wild-type MEFs until about 18 h posttreatment; Cdc20 in these cells then returned to a level lower than that in wild-type MEFs (Fig. 1*C*, 18 h and beyond). Moreover, a significant fraction of BubR1 in wild-type MEFs, but not in *BubR1*$^{+/-}$ MEFs, was phosphorylated on nocodazole treatment, and the phosphorylation peaked between 14 and 18 h posttreatment. On the other hand, Mad2 levels in *BubR1*$^{+/-}$ MEFs were not significantly modulated in the presence or absence of nocodazole.

To confirm that *BubR1* deficiency directly caused a reduction of securin, we examined securin levels in HeLa cells transfected with siRNAs targeting human *BubR1* or luciferase (as a negative control). *BubR1* siRNA, but not control one, effectively down-regulated BubR1 expression 3 days after transfection (Fig. 1*D*). Consistently, the securin level was also significantly reduced. By day 5, securin had almost completely disappeared from HeLa cells transfected with siRNA targeting *BubR1*.

To determine whether mitosis was affected in *BubR1*$^{+/-}$ MEFs, we examined the percentage of cells positive for phosphorylated histone H3, a mitotic marker tightly associated with chromosome condensation (Fig. 2*A*). Fluorescence microscopy revealed that there existed significantly fewer phosphorylated histone H3-positive cells in *BubR1*$^{+/-}$ MEFs than in wild-type MEFs (Fig. 2*B*). About 3.8% of *BubR1*$^{+/-}$ MEFs were in mitotic stages as revealed by phosphorylated histone H3 staining, whereas 9.2% of cells were mitotic in wild-type MEFs (Fig. 2*C*). Chromosome mis-segregation and micronuclei formation are hallmarks of a compromised spindle checkpoint (7). A greatly increased number of *BubR1*$^{+/-}$ MEF cells contained spontaneously formed micronuclei compared with the wild-type MEFs (Fig. 2, *D* and *E*). Irregular nuclear shape and nuclear blebbing were also observed in *BubR1*$^{+/-}$ MEFs (data not shown).

Because mutations of the *BubR1* gene were first identified in human colon cancer cells (8) and because BubR1 is epigenetically down-regulated in a substantial fraction of human cancers (9), we investigated whether *BubR1*$^{+/-}$ mice were more susceptible to carcinogenesis after treatment with AOM, a colon carcinogen. Wild-type mice typically develop a low incidence of colonic tumors 6–8 months after initiation of AOM treatment (12). About 2 months after the completion of AOM treatment, *BubR1*$^{+/-}$ mice had already exhibited abnormal and dilated crypts (data not shown). These mice subsequently developed a significant number of microadenomas and adenoma-like masses (Fig. 3*B*; Table 1). Polyps were scarcely detected in colons of wild-type C57/BL6 mice at this stage of treatment (Table 1), however. Histological studies revealed that when compared with the

[1] Wei Dai and Tongyi Liu, unpublished data.

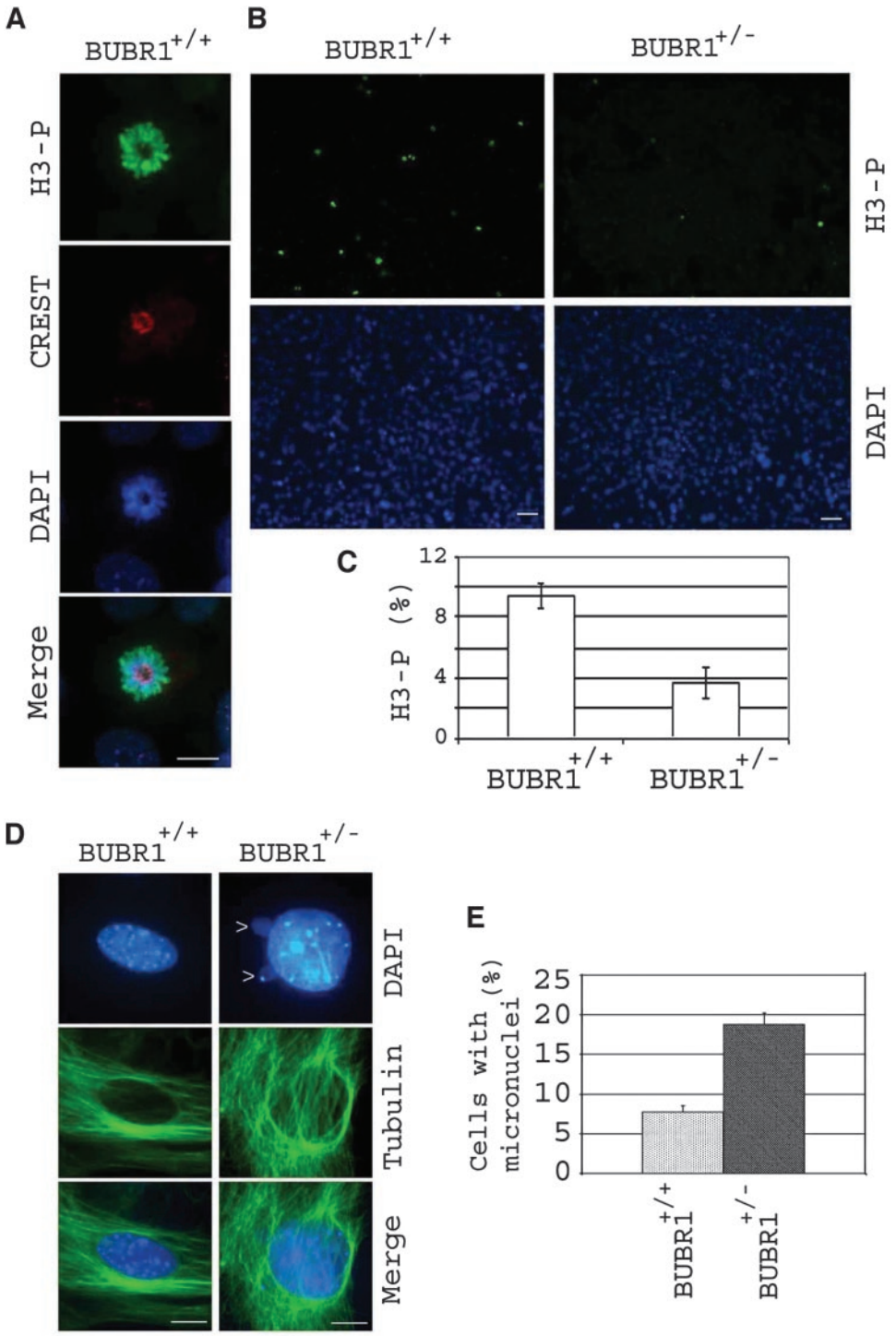

Fig. 2. Mitotic slippage associated with abnormal nuclear morphology in *BubR1*$^{+/-}$ deficient cells. *A*, wild-type mouse embryonic fibroblasts (MEFs) fixed and stained with antibodies to phosphorylated histone H3 (*H3-P*; *green*) or kinetochore antigen CREST (*red*) were examined by fluorescence microscopy. DNA was stained with 4′,6-diamidino-2-phenylindole. A typical prophase cell strongly stained with phosphorylated histone H3 is shown. *Bar*, 10 μm. *B*, *BubR1*$^{+/-}$ and wild-type MEFs fixed and stained with an antibody to phosphorylated histone H3 (*green*, *top panels*) and 4′,6-diamidino-2-phenylindole (*blue*, *bottom panels*). *Bar*, 50 μm. *C*, both *BubR1*$^{+/-}$ and wild-type MEFs positive for phosphorylated histone H3 were scored from 500 cells, and the percentage of the positive cells is shown. *D*, *BubR1*$^{+/-}$ and wild-type MEFs stained with antibody to α-tubulin and 4′,6-diamidino-2-phenylindole were examined by fluorescence microscopy. *Arrows* denote micronuclei. *Bar*, 5 μm. *E*, micronuclei formed in both *BubR1*$^{+/-}$ and wild-type MEFs were scored from 500 cells; the percentage of cells with micronuclei is shown.

normal structure of colon, these polyps were indeed neoplastic (Table 1; Fig. 3, *C* and *D*). Colonic tubular adenomas were lined with mild dysplastic epithelium, and glands exhibited partial loss of polarity with a mild architecture distortion (Fig. 3*C*). Based on common pathological criteria (*e.g.*, gland architecture, nuclear/cytoplasmic ratio, nuclear location, and amount of interglandular stroma), many large tumors from *BubR1*$^{+/-}$ animals were classified as well to moderately differentiated adenocarcinomas with complex and highly packed glands (Fig. 3*D*).

We next examined several other major organs (*e.g.*, spleen, liver, and lung) for any sign of tumor formation. No neoplastic growths were detected in either *BubR1*$^{+/-}$ or wild-type spleens. To our surprise, *BubR1*$^{+/-}$ mice, but not the wild-type mice, developed many lung adenocarcinomas (Fig. 4*A*) as well as neoplasm in liver (data not shown). Tumor masses were typically well circumscribed, but not encapsulated, and situated at the periphery of the lung. They exhibited hyperchromatic and pleomorphic nuclei with abundant eosinophilic cytoplasm. Consistent with pulmonary adenocarcinoma, some tumor cells apparently formed glands with a lumen, whereas others formed trabecular patterns (Fig. 4*A*). Immunohistochemical studies revealed that lung adenocarcinomas were strongly stained with proliferative cell nuclear antigen (Fig. 4*B*), indicating that these tumor cells were

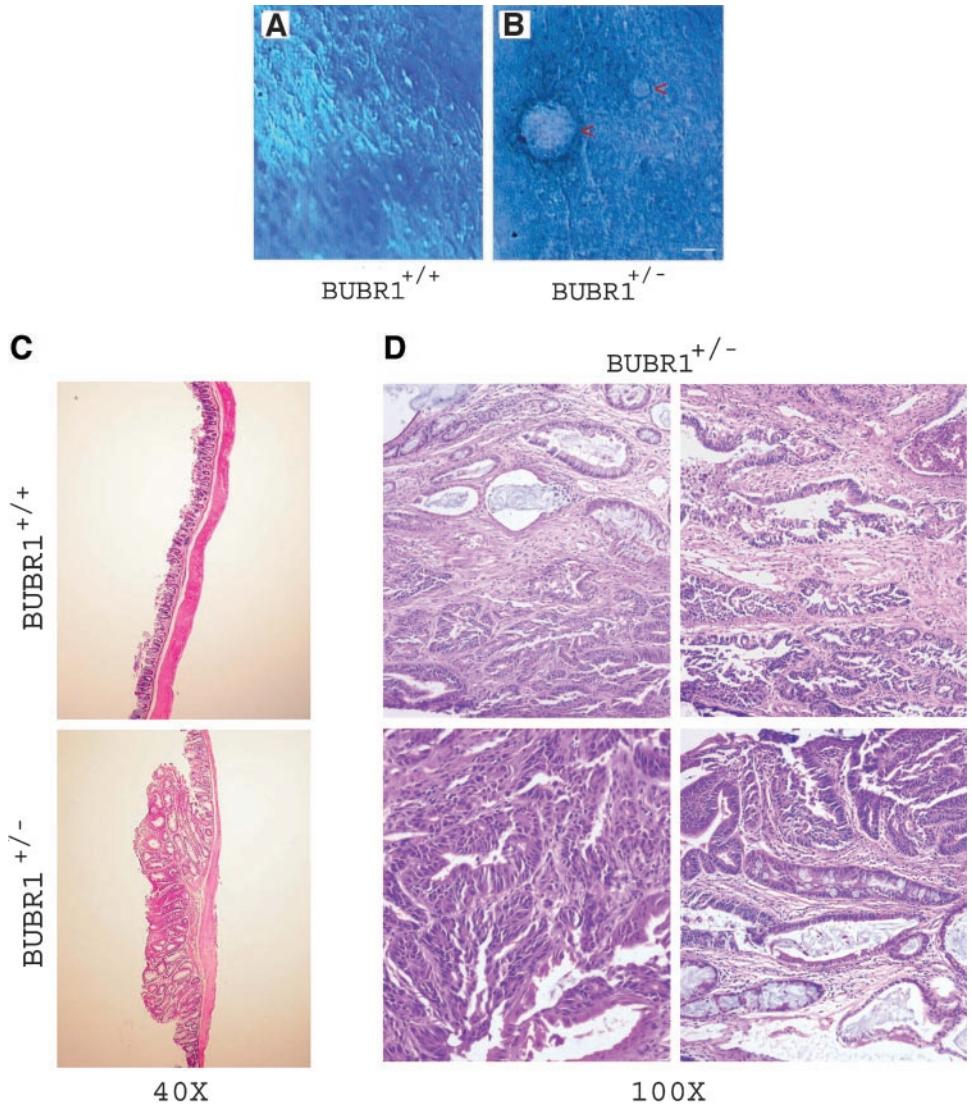

Fig. 3. *BubR1*$^{+/-}$ mice are more susceptible to the development of intestinal tumors. Both *BubR1*$^{+/-}$ and wild-type mice were treated with azoxymethane (AOM) for 5 weeks as described in "Materials and Methods." *A* and *B*, 8 weeks after AOM treatment, colons from individual mice were collected and stained with methylene blue. A topographical view of a typical wild-type colon section is shown in *A*, and a similar colon section with abnormal masses from a *BubR1*$^{+/-}$ mouse is shown in *B*. *Arrows* indicate focal of adenoma-like masses observed only in *BubR1*$^{+/-}$ mice. All images were obtained with a ×4 lens. *Bar*, 2 mm. *C*, H&E-stained colon sections from *BubR1*$^{+/+}$ and *BubR1*$^{+/-}$ mice treated with AOM (magnification, ×40). A colonic adenoma from *BubR1*$^{+/-}$ mice treated with AOM appears in the *bottom panel*. *D*, H&E-stained sections of various adenocarcinomas from *BubR1*$^{+/-}$ mice treated with AOM (magnification, ×100).

highly proliferative. The susceptibility of *BubR1*$^{+/-}$ mice to lung tumor formation after challenge with the colon carcinogen AOM is unexpected because C57/BL6 mice are very resistant to the development of tumors, even when the lung-specific carcinogens such as 4-(methylnitrosamino)-1-(3-pyridyl)-1-butanone are used. It is intriguing to note that lung appears prone to development of cancer when the spindle checkpoint is compromised because Mad2 or Bub3 haploinsufficiency also results in enhanced development of lung cancer (13, 14).

Discussion

Extensive biochemical and molecular analyses have shown that BubR1 plays a central role in spindle checkpoint activation (5, 15, 16). It both coordinates the interaction of Bub3, Mad1, Mad2, and CENP-E with kinetochores and contributes to inhibition of APC activity during activation of this checkpoint. The APC is an E3 ubiquitin ligase that mediates the polyubiquitination of securin, thereby targeting it for degradation by the proteosome (16). Securin binds to and inhibits the proteolytic activity of separase, which destroys the link between sister chromatids by cleaving the chromatid cohesin factor Scc1. Degradation of securin is required for the separation of sister chromatids during mitosis. Reduced levels of securin in *BubR1*$^{+/-}$ MEFs are closely correlated with *BubR1* deficiency as well as with its activation status (Fig. 1*C*). Moreover, down-regulation of BubR1 via RNA interference resulted in almost complete disappearance of securin (Fig. 1*D*), strongly suggesting that BubR1 plays a pivotal role in the inhibition of APC during spindle checkpoint activation. In fact, enhanced genetic instability (*e.g.*, polyploidy and micronuclei formation) in *BubR1*$^{+/-}$ MEF cells correlates very well with the observation that securin$^{-/-}$ cells lose chromosomes with a high frequency (17).

Table 1 *Effect of azoxymethane on tumor formation in wild-type and BubR1*$^{+/-}$ *mice*

Experimental group	Microadenomas (<1.5 mm)[a]	Adenomas[b]	Adenocarcinomas
BubR1$^{+/+}$ mice	0.4 ± 0.2[c]	0 ± 0	0 ± 0
BubR1$^{+/-}$ mice	7.2 ± 1.1	2.6 ± 0.7	1.2 ± 0.4

[a] Direct microscopic observation.
[b] Histological evaluation.
[c] Mean ± SE (N = 10).

It is believed that one of the consequences of the loss of spindle checkpoint is genetic instability of the resulting daughter cells, which predisposes these cells to malignant transformation. Some evidence indicates that structural alterations or a loss of functional spindle checkpoint components may trigger certain cancers because mutations have been detected in *Bub1* and *BubR1* (8, 18). Although we have not

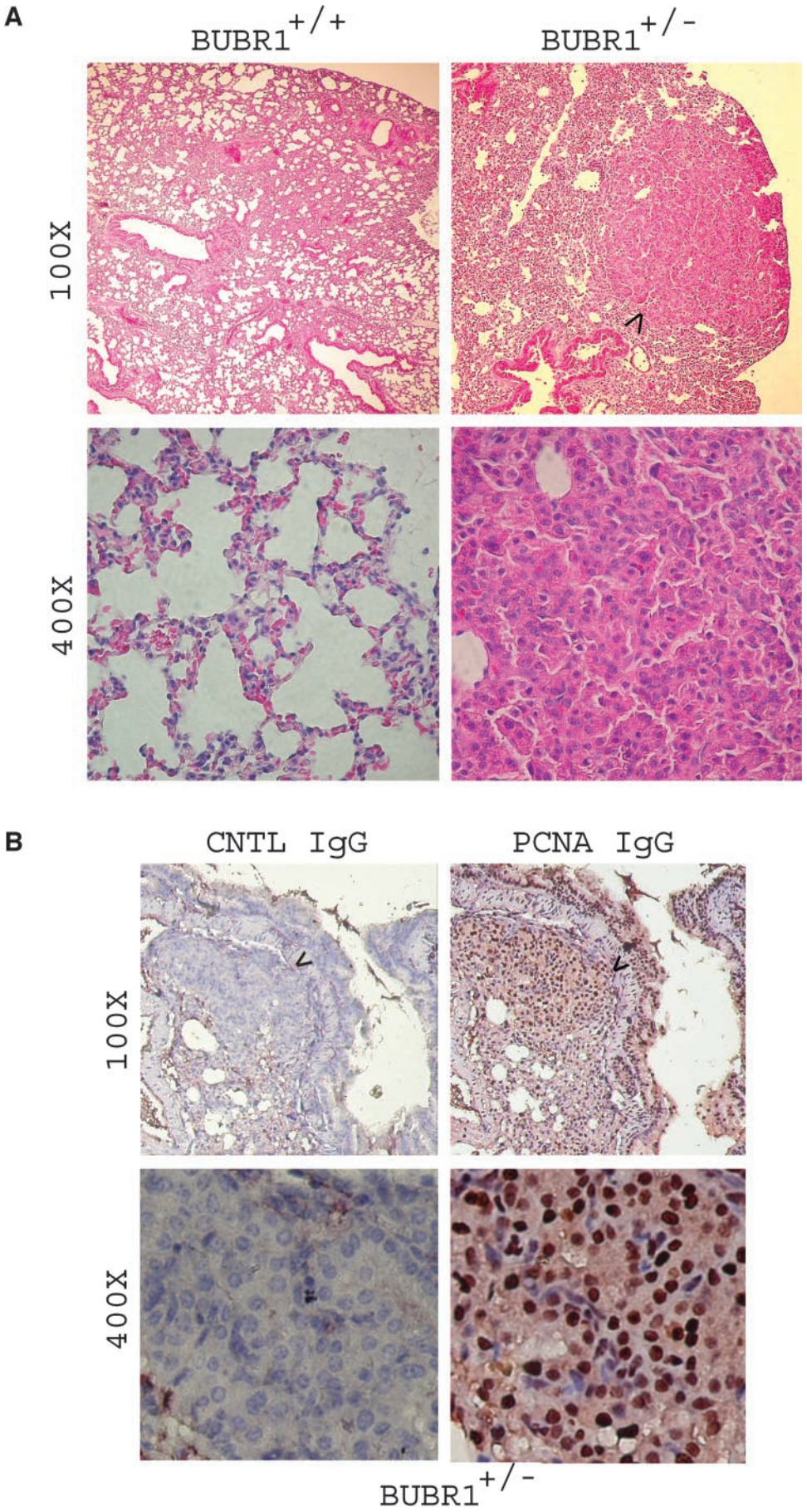

Fig. 4. *BubR1*$^{+/-}$ mice, but not wild-type mice, develop lung adenomas after exposure to azoxymethane. *A*, lung sections from *BubR1*$^{+/+}$ and *BubR1*$^{+/-}$ mice treated with azoxymethane for 12 weeks were stained with H&E (magnifications, ×100 and ×400, respectively). *Arrow* indicates a solitary tumor mass in *BubR1*$^{+/-}$ lung; the region is subjected to high-power magnification. *B*, neighboring sections of the same lung tissue from *BubR1*$^{+/-}$ mice were subjected to immunohistochemical studies after staining with either control immunoglobulin (*IgG*) or proliferative cell nuclear antigen IgG (magnifications, ×100). *Arrows* indicate a solitary tumor; the same region is subjected to high-power magnification (×400).

observed a significant increase in spontaneous tumors in *BubR1*$^{+/-}$ mice, our recent studies have demonstrated that these mice are prone to the development of neoplastic lesions of colon and lung within 2 months after they have been challenged with the carcinogen. In contrast, neither lesion is detected in wild-type mice at the same treatment stage, suggesting that *BubR1* is a tumor susceptibility gene. Consistently, recent *in vitro* studies show that adenomatous polyposis coli protein plays an important role in chromosomal segregation by interacting with BubR1 and that defects in adenomatous polyposis coli lead to increased chromosomal instability (19), underscoring the importance of further exploration of the role of *BubR1* in colon cancer using this animal model. Intriguingly, it is expected that a significantly compromised spindle checkpoint observed with *BubR1*$^{+/-}$ MEF cells would conceivably lead to widespread aneuploidy and rapid development of spontaneous tumors in the transgenic animals. Our explanations are as follows: (*a*) the spindle checkpoint in *BubR1*$^{+/-}$ cells is compromised, but not completely failed; and (*b*) animals are capable of elimination of most cells with severe chromosomal instabilities through apoptosis. This mechanism would prevent the early onset of tumors until a second insult occurs during aging or under a carcinogen stress. This view is supported by the facts that haploinsufficiency of *Mad2* and *Bub3/Rae1* results in a significantly enhanced lung cancer incidence in aging (beyond 18 months; Ref. 13) and carcinogen-challenged (20) mice, respectively.

In this study, we have addressed an *in vivo* role of *BubR1* by using a mouse gene knockout approach. *BubR1* haploinsufficiency results in a compromised spindle checkpoint, leading to slippage of mitotic arrest. A recent study shows that CENP-E functions as an activator of the essential checkpoint kinase BubR1; inactivation of BubR1 kinase activity silences the signaling of the spindle checkpoint (6). Thus, the availability of *BubR1*$^{+/-}$ mice should now greatly facilitate characterization of the functional interactions between BubR1 and various spindle checkpoint components, including CENP-E, Mad2, and other spindle checkpoint gene products.

Acknowledgments

We thank Dr. Robert Benezra and Dr. Jasminder Weinstein for Mad2 and Cdc20 antibodies, respectively. We are also grateful to Drs. Rulong Shen and Chung-Xiong Wang for discussions and valuable input about mouse histology. We also thank Dr. C. Clifford Conaway for reading the manuscript.

References

1. Li, W., Lan, Z., Wu, H., Wu, S., Meadows, J., Chen, J., Zhu, V., and Dai, W. BUBR1 phosphorylation is regulated during mitotic checkpoint activation. Cell Growth Differ., *10:* 769–775, 1999.
2. Sudakin, V., Chan, G. K., and Yen, T. J. Checkpoint inhibition of the APC/C in HeLa cells is mediated by a complex of BUBR1, BUB3, CDC20, and MAD2. J. Cell Biol., *154:* 925–936, 2001.
3. Chen, R. H. BubR1 is essential for kinetochore localization of other spindle checkpoint proteins and its phosphorylation requires Mad1. J. Cell Biol., *158:* 487–496, 2002.
4. Shannon, K. B., Canman, J. C., and Salmon, E. D. Mad2 and BubR1 function in a single checkpoint pathway that responds to a loss of tension. Mol. Biol. Cell, *13:* 3706–3719, 2002.
5. Hoyt, M. A. A new view of the spindle checkpoint. J. Cell Biol., *154:* 909–911, 2001.
6. Mao, Y., Abrieu, A., and Cleveland, D. W. Activating and silencing the mitotic checkpoint through CENP-E-dependent activation/inactivation of BubR1. Cell, *114:* 87–98, 2003.
7. Rajagopalan, H., Nowak, M. A., Vogelstein, B., and Lengauer, C. The significance of unstable chromosomes in colorectal cancer. Nat. Rev. Cancer, *3:* 695–701, 2003.
8. Cahill, D. P., Lengauer, C., Yu, J., Riggins, G. J., Willson, J. K., Markowitz, S. D., Kinzler, K. W., and Vogelstein, B. Mutations of mitotic checkpoint genes in human cancers. Nature (Lond.), *392:* 300–303, 1998.
9. Shichiri, M., Yoshinaga, K., Hisatomi, H., Sugihara, K., and Hirata, Y. Genetic and epigenetic inactivation of mitotic checkpoint genes hBUB1 and hBUBR1 and their relationship to survival. Cancer Res., *62:* 13–17, 2002.
10. Rao, C. V., Desai, D., Simi, B., Kulkarni, N., Amin, S., and Reddy, B. S. Inhibitory effect of caffeic acid esters on azoxymethane-induced biochemical changes and aberrant crypt foci formation in rat colon. Cancer Res., *53:* 4182–4188, 1993.
11. Wang, Q., Liu, T-Y., Fang, Y-Q., Xie, S-Q., Huang, X., Ramashiwamy, G., Sakamoto, K., Dayzynkiewicz, Z., Xu, M., and Dai, W. *BUBR1* deficiency results in abnormal megakaryopoiesis. Blood, in press, 2004.
12. Csuka, O., Szentirmay, Z., and Sugar, J. The effect of promoters on 1,2-dimethylhydrazine-induced colon carcinogenesis. IARC Sci. Publ., *56:* 129–136, 1984.
13. Michel, L. S., Liberal, V., Chatterjee, A., Kirchwegger, R., Pasche, B., Gerald, W., Dobles, M., Sorger, P. K., Murty, V. V., and Benezra, R. MAD2 haplo-insufficiency causes premature anaphase and chromosome instability in mammalian cells. Nature (Lond.), *409:* 355–359, 2001.
14. Babu, J. R., Jeganathan, K. B., Baker, D. J., Wu, X., Kang-Decker, N., and van Deursen, J. M. Rae1 is an essential mitotic checkpoint regulator that cooperates with Bub3 to prevent chromosome missegregation. J. Cell Biol., *160:* 341–353, 2003.
15. Chan, G. K., Jablonski, S. A., Sudakin, V., Hittle, J. C., and Yen, T. J. Human BUBR1 is a mitotic checkpoint kinase that monitors CENP-E functions at kinetochores and binds the cyclosome/APC. J. Cell Biol., *146:* 941–954, 1999.
16. Musacchio, A., and Hardwick, K. G. The spindle checkpoint: structural insights into dynamic signalling. Nat. Rev. Mol. Cell Biol., *3:* 731–741, 2002.
17. Jallepalli, P. V., Waizenegger, I. C., Bunz, F., Langer, S., Speicher, M. R., Peters, J. M., Kinzler, K. W., Vogelstein, B., and Lengauer, C. Securin is required for chromosomal stability in human cells. Cell, *105:* 445–457, 2001.
18. Reis, R. M., Nakamura, M., Masuoka, J., Watanabe, T., Colella, S., Yonekawa, Y., Kleihues, P., and Ohgaki, H. Mutation analysis of hBUB1, hBUBR1 and hBUB3 genes in glioblastomas. Acta Neuropathol. (Berl.), *101:* 297–304, 2001.
19. Kaplan, K. B., Burds, A. A., Swedlow, J. R., Bekir, S. S., Sorger, P. K., and Nathke, I. S. A role for the adenomatous polyposis coli protein in chromosome segregation. Nat. Cell Biol., *3:* 429–432, 2001.
20. Meyn, M. S. Ataxia-telangiectasia and cellular responses to DNA damage. Cancer Res., *55:* 5991–6001, 1995.

Slippage of Mitotic Arrest and Enhanced Tumor Development in Mice with *BubR1* Haploinsufficiency

Wei Dai, Qi Wang, Tongyi Liu, et al.

Cancer Res 2004;64:440-445.